

# The thermal expansion behaviour of oriented polypropylene

S. A. Jawad\*, G. A. J. Orchard and I. M. Ward

Department of Physics, University of Leeds, Leeds LS2 9JT, UK

(Received 18 November 1985; revised 6 March 1986)

The thermal expansion behaviour of die drawn polypropylene rods has been measured over the temperature range  $-50^{\circ}\text{C}$  to  $+10^{\circ}\text{C}$ . For high draw samples the values for the thermal expansion coefficient in the axial direction  $\alpha_{\parallel}$  are negative and increase in magnitude with increasing temperature. It is shown that this result is consistent with the presence of an internal shrinkage stress. For low draw samples and most high draw samples after annealing, the value of  $\alpha_{\parallel}$  is positive and increases in magnitude with increasing temperature. It is shown that this result can also be explained in terms of an internal shrinkage stress, on the basis of a simple relationship between the axial and radial expansion coefficients.

(Keywords: thermal expansion; shrinkage force; drawn polypropylene)

## INTRODUCTION

In common with other physical properties, the thermal expansion behaviour of oriented polymers shows marked anisotropy. In particular, there are substantial changes in the behaviour in the major orientation direction (the draw direction for an oriented polymer produced by drawing) as drawing proceeds. This contrasts with much smaller changes in the transverse direction. It is well established that many highly oriented polymers show a negative coefficient of thermal expansion in the draw direction and a positive coefficient in the transverse direction. There are two theoretical attempts to explain this negative expansivity. Choy *et al.*<sup>1</sup> have proposed that it relates directly to the presence of tie molecules which produce a contraction at high temperatures whereas Orchard *et al.*<sup>2</sup>, in a more recent publication, have suggested that it relates to the presence of a frozen-in stress, which becomes more effective at high temperatures due to the fall in the tensile modulus with increasing temperature. It was shown that this model could give a satisfactory quantitative explanation of the results for highly oriented polyethylene, and predict a value for the frozen-in stress which agreed well with the shrinkage force observed at high temperatures.

In this paper the behaviour of a series of oriented polypropylene samples is described. The results emphasize the differences in structure which can occur for different preparation conditions and also when internal stresses are relieved by annealing. It is shown that the theoretical modelling proposed previously by Orchard *et al.* is applicable for the most highly oriented polypropylene. The less well oriented samples show somewhat different behaviour which requires an extension of the theoretical model to allow for the intrinsic variation of thermal expansion coefficient with temperature. It will be shown that this revised model provides a satisfactory interpretation of the results for low draw samples at a phenomenological level of understanding.

\* Permanent address: University of United Arab Emirates, Physics Department, Al-Ain, U.A.E.

## EXPERIMENTAL

### Sample preparation

The polymer used was Propathane GSE 108,  $MFI=0.8$ , a polypropylene copolymer manufactured by ICI plc. Samples were prepared by a die drawing technique which has been described in detail in a previous publication<sup>3</sup>. Briefly, isotropic rod machined from a cast billet was drawn through a heated 4 mm die at various drawing speeds to obtain a range of molecular orientations. The draw temperature was controlled at  $110^{\circ}\text{C}$  to an accuracy of  $\pm 1^{\circ}\text{C}$ . Further control of the draw ratio could be achieved by varying the diameter of the isotropic feedstock billet so that the draw ratio of the extruded rod as determined by the change in area could be varied between 2.4 and 16.8. Details of the various samples are shown in Table 1.

Annealing was carried out either at  $115^{\circ}\text{C}$  or at  $130^{\circ}\text{C}$ . The annealing treatment varied. In some cases the samples were enclosed in a glass tube and the tube immersed in a silicone oil bath controlled at the required temperature. For these samples the annealing time was two hours and the sample was left in the oil bath to cool slowly to room temperature. For other samples more

Table 1 Production conditions for polypropylene die drawn rods with die diameter 4 mm at  $110^{\circ}\text{C}$  draw temperature

	Draw ratio	Draw speed (mm/min)	Feedstock diameter (mm)	1 min Creep modulus at $15^{\circ}\text{C}$ (GPa)
Set 1	3.9	10	6.9	—
	6.4	10	8.9	8.0
	8.9	10	10.6	9.0
	10.7	50	10.6	10.8
	12.7	100	10.6	12.5
	16.8	200	10.6	15.0
Set 2	2.4	150	6.4	1.5
	6.2	150	7.6	3.6
	9.6	150	8.5	6.6
	12.6	150	9.4	10.2

immediate annealing was achieved with a 10 min treatment in a hot air stream controlled at the required temperature. In most cases the samples were annealed unconstrained. Individual samples where shrinkage was prevented are considered in a later section.

*Thermal expansion measurements*

Thermal expansion measurements were made on equipment developed in our laboratory, and further details are given in a previous publication<sup>2</sup>.

The thermal expansion measurements were carried out on extruded rods over six temperature ranges, covering a mean temperature range from  $-51^{\circ}\text{C}$  to  $+9^{\circ}\text{C}$ .

The measurements were made on both as-drawn and annealed samples in two directions, parallel and perpendicular to the draw direction.

*Creep modulus measurements*

The one minute isochronal creep modulus was measured in the temperature range  $-60^{\circ}\text{C}$  to  $+20^{\circ}\text{C}$ . The modulus was determined from a three point bend test with a sample length of about 15 cm. In this test the sample is supported horizontally at two points and a load is applied at the centre. Surrounding the sample was a polyurethane foam chamber. This was supplied with cold gas boiled off from a dewar of liquid nitrogen. The nitrogen gas passed over a heater coil controlled by a Eurotherm proportional temperature controller. The sample temperature was maintained to an accuracy of about  $\pm 0.5^{\circ}\text{C}$  over the temperature range  $-60^{\circ}\text{C}$  to  $+20^{\circ}\text{C}$ .

RESULTS

The thermal expansion coefficients parallel to the draw direction,  $\alpha_{||}$ , for the samples from set 1 (see Table 1) are plotted against temperature in Figure 1 for the various draw ratios. Corresponding values obtained after unconstrained annealing in air at  $115^{\circ}\text{C}$  or at  $130^{\circ}\text{C}$  are shown in Figures 2 and 3 respectively.

Before annealing, the parallel coefficient decreases rapidly with draw ratio, as can be seen in Figure 4, becomes zero at about draw ratio 6 and thereafter decreases more slowly to about  $-11 \times 10^{-6} \text{ K}^{-1}$ . After annealing the values are higher with greater changes at the higher annealing temperature. For a draw ratio of 6.4 the parallel expansion coefficient is positive after annealing at  $115^{\circ}\text{C}$  whereas it is necessary to anneal at  $130^{\circ}\text{C}$  to achieve the same effect with the draw ratios of 8.9 and 10.7. At higher draw ratios the changes are smaller. The magnitudes obtained whether positive or negative are generally lower at lower temperatures. This result is similar to that reported by Choy *et al.*<sup>4</sup>.

The expansion coefficient in the radial direction increases on initial drawing but thereafter remains almost constant with only a slight decline as the draw ratio is increased (Figure 4). There is a marked dependence on temperature as shown in Figures 5, 6 and 7 for the drawn rods and for the high and low draw ratio samples annealed at  $115^{\circ}\text{C}$  and  $130^{\circ}\text{C}$  respectively. The temperature variability is similar for all the drawn samples both before and after annealing.

The second set of samples, set 2, was prepared under slightly different conditions with a constant draw speed and different feedstock diameters to obtain various draw

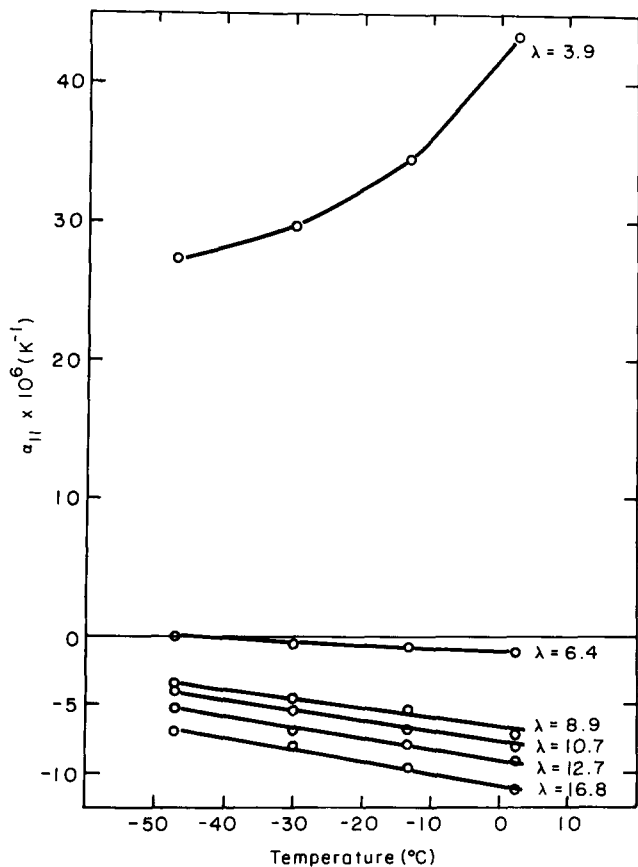


Figure 1 Variation with temperature of the thermal expansion coefficient parallel to the draw direction for polypropylene rods from set 1 at various draw ratios

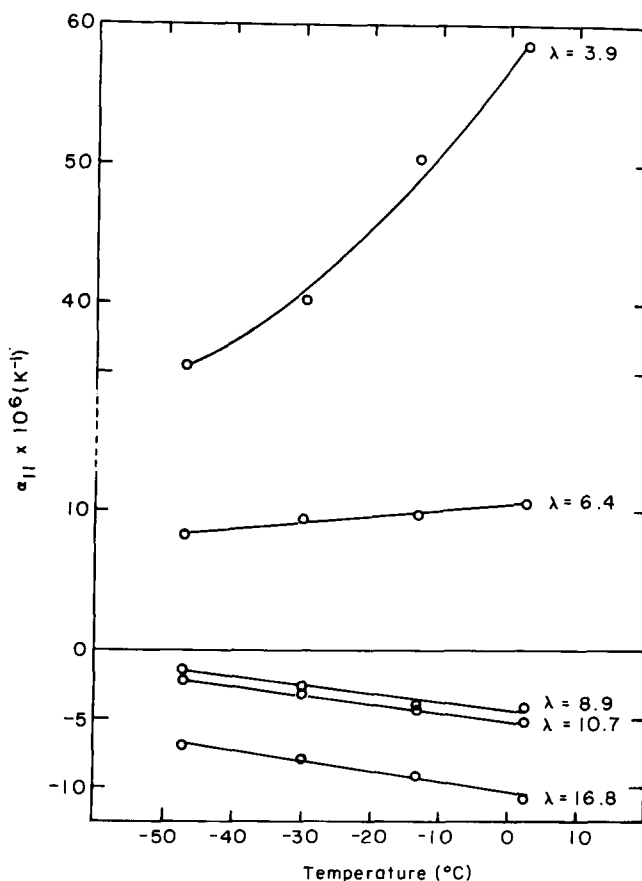


Figure 2 Effect of unconstrained annealing in air at  $115^{\circ}\text{C}$  on the thermal expansion coefficient parallel to the draw direction

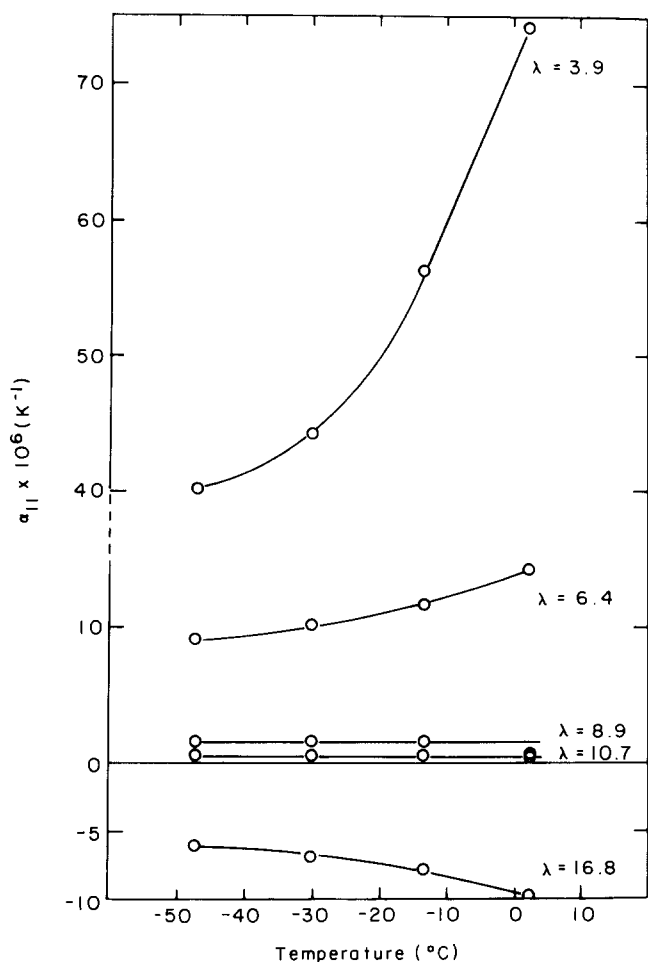


Figure 3 Effect of unconstrained annealing in air at 130°C on the thermal expansion coefficient parallel to the draw direction

ratios. The samples were held under tension after drawing for a period of 20 min. The rods obtained were found to have lower creep modulus values, as determined by a 1 minute three point bend test, and consequently lower orientation than samples with similar draw ratios in set 1. Similarly the expansion coefficients for measurements parallel to the draw direction (Figure 8) are higher for set 2 than for corresponding draw ratios in set 1. The values obtained for a draw ratio of 6.2 are now positive before annealing. After annealing which was carried out for an extended period in an oil bath at 130°C, the expansion coefficients are all positive (Figure 9). In the transverse direction both sets of samples show similar temperature variability both before and after annealing.

## DISCUSSION

The influence of the drawing process on the thermal expansion coefficient of both amorphous and semicrystalline polymers has been extensively studied. The anisotropy and the changes in the orientation of the structure have been found to cause significant differences between measurements parallel and perpendicular to the draw direction. In particular there are several instances where the expansion coefficient along the draw direction decreases and becomes negative with increasing draw ratio as has been observed in the current measurements.

It has been suggested that, apart from any intrinsic crystalline contribution, a significant part of the negative

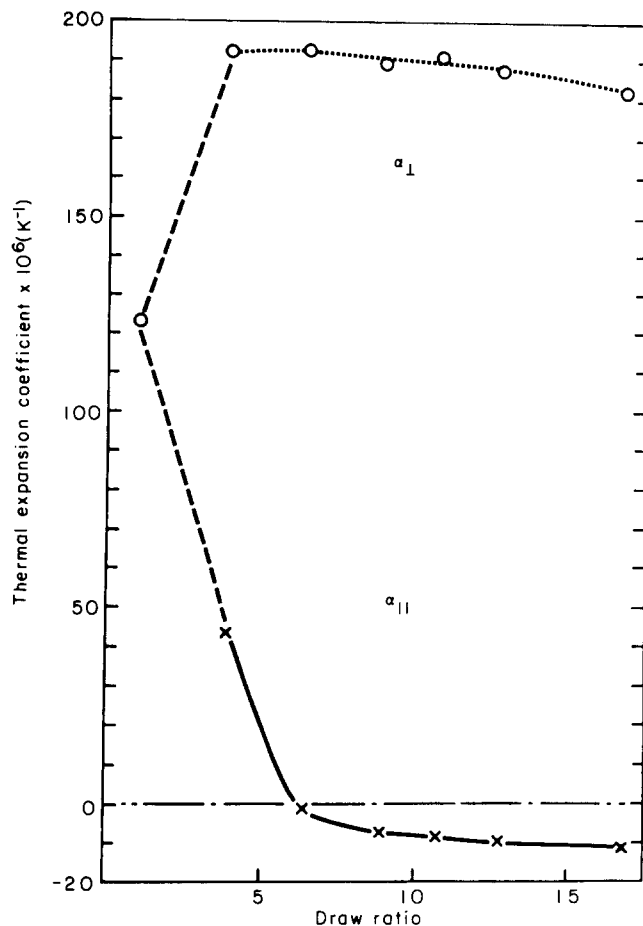


Figure 4 Variation with draw ratio of the thermal expansion coefficients of polypropylene die drawn rods parallel and perpendicular to the draw direction

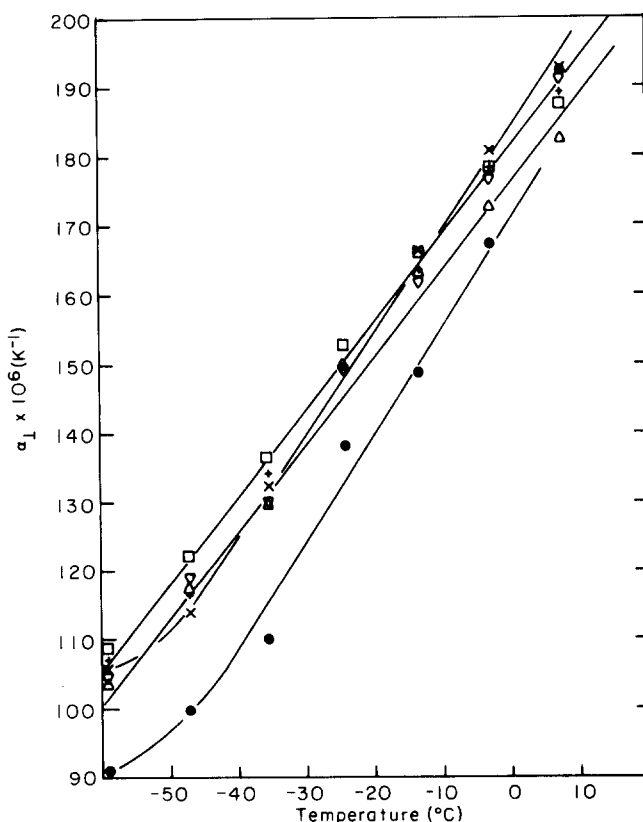


Figure 5 Variation with temperature of the thermal expansion coefficient perpendicular to the draw direction for polypropylene rods from set 1 at various draw ratios. Key to draw ratios: (●) 3.9; (×) 6.4; (+) 8.9; (▽) 10.7; (□) 12.7; (△) 16.8

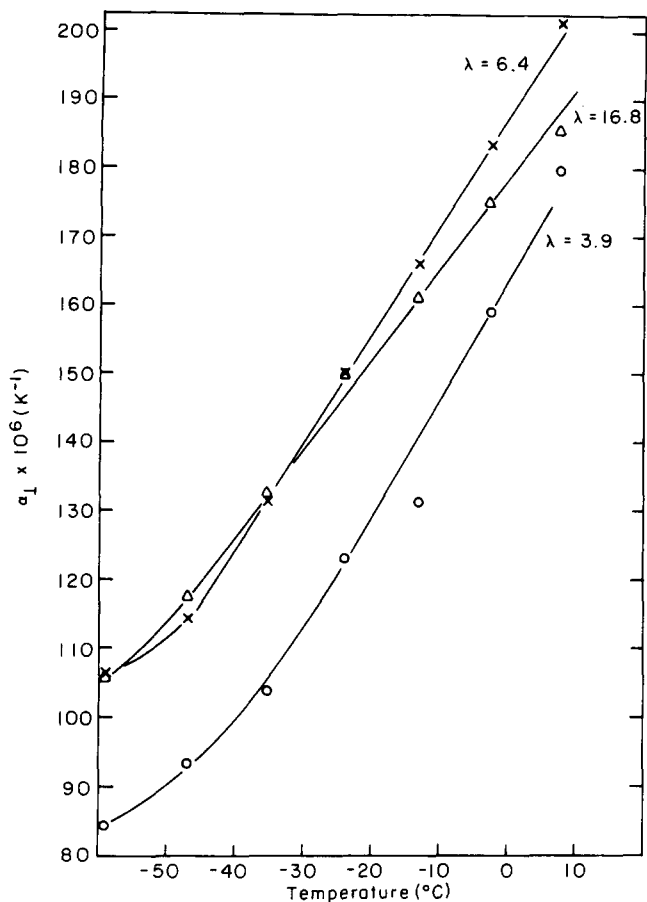


Figure 6 Effect of unconstrained annealing in air at 115°C on the thermal expansion coefficient perpendicular to the draw direction

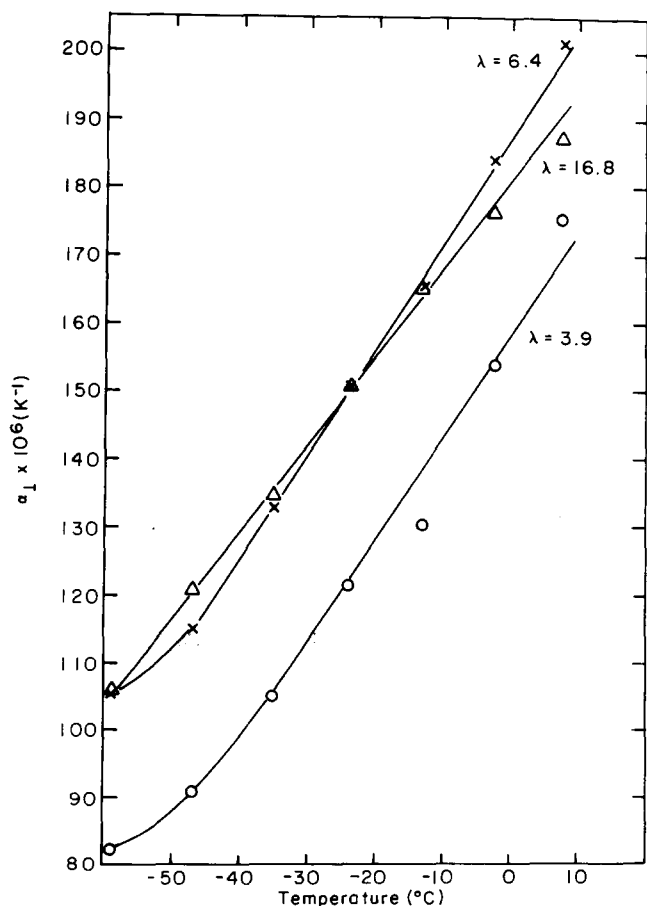


Figure 7 Effect of unconstrained annealing in air at 130°C on the thermal expansion coefficient perpendicular to the draw direction

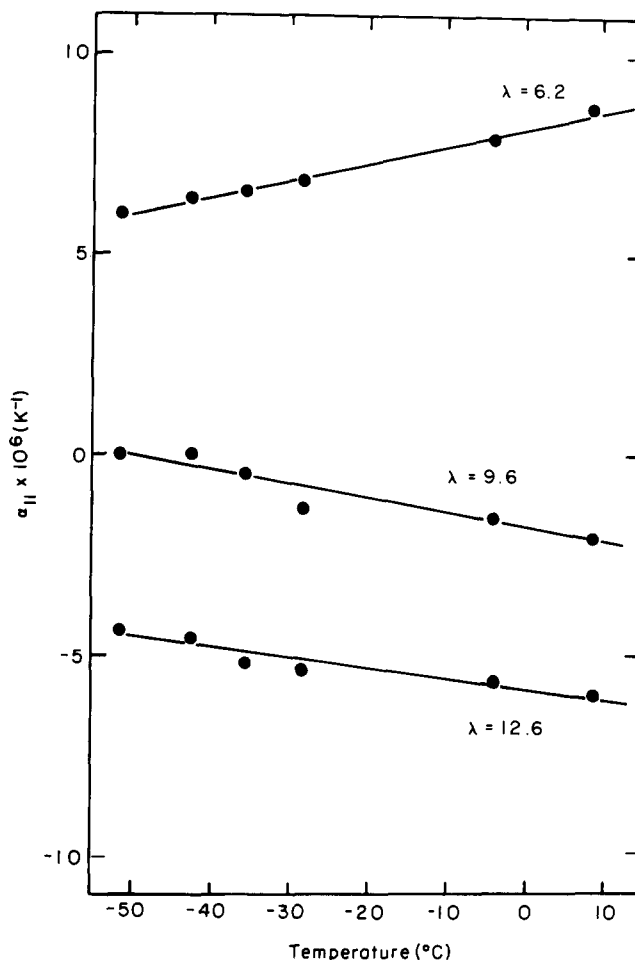


Figure 8 Variation with temperature of the thermal expansion coefficient parallel to the draw direction for polypropylene rods from set 2 at various draw ratios

thermal expansion coefficients obtained for highly oriented polymers arises from the effect of entropic internal stresses in the amorphous regions<sup>5</sup>. In a recent publication<sup>2</sup> the following expression has been derived which relates the thermal expansion behaviour to the change in tensile modulus  $E$  with absolute temperature  $T$  and the frozen-in stress

$$\alpha_{\parallel} - \alpha_0 = \frac{B}{E} \left[ \frac{T}{E} \frac{dE}{dT} - 1 \right] \quad (1)$$

where  $\alpha_0$  is the intrinsic thermal expansion coefficient and  $B = -\sigma/T$  is the shrinkage stress per degree Kelvin which depends on the parameters of the network. This equation predicts that if the measured thermal expansion coefficients,  $\alpha_{\parallel}$ , at various temperatures are plotted against the corresponding values of

$$\frac{1}{E} \left[ \frac{T}{E} \frac{dE}{dT} - 1 \right]$$

a straight line will be obtained with a slope of  $B$  and an intercept on the expansion axis of  $\alpha_0$ .

Applying equation (1) to the higher draw ratio samples in set 1 with the one minute modulus values for  $E$ , reasonably linear relationships are obtained as shown in Figure 10 to give values of  $B$  ranging between 0.010 MPa/K for draw ratio 8.9 and 0.032 MPa/K for

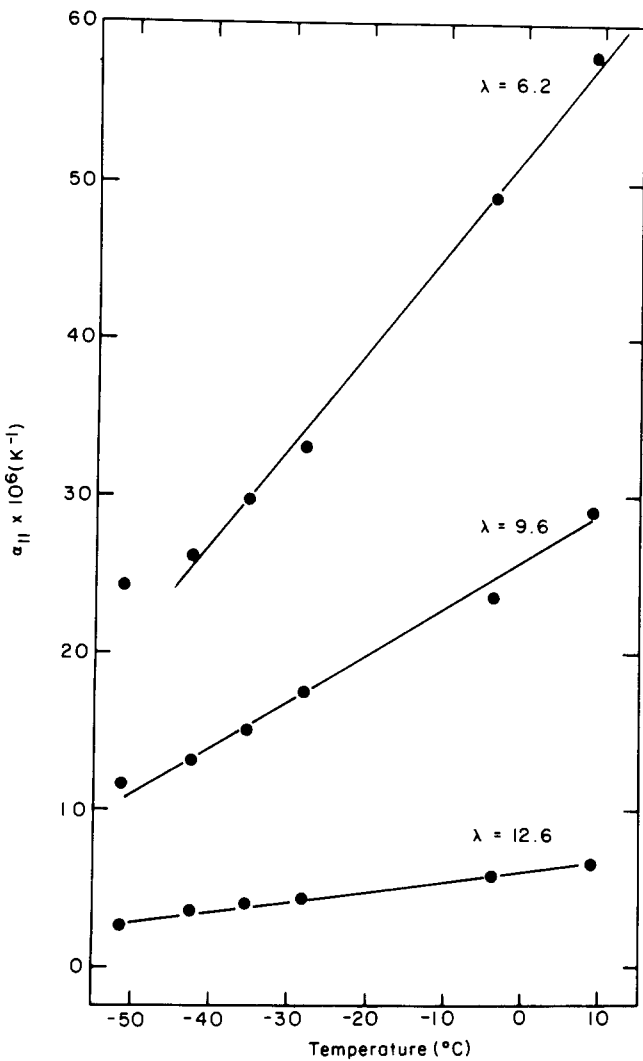


Figure 9 Effect of unconstrained annealing in an oil bath at 130°C on the longitudinal expansion coefficient of samples from set 2

draw ratio 16.8 with intercepts between  $-2.6 \times 10^{-6} \text{ K}^{-1}$  and  $-4.5 \times 10^{-6} \text{ K}^{-1}$ . Direct measurements of the shrinkage stress developed in the rods when they are immersed in a hot oil bath at 115°C have been made with equipment described in a previous publication<sup>2</sup>. The results are given in the final column of Table 2 for comparison with those calculated from the values for  $B$ . The shrinkage stress for the highest draw ratio is lower than expected but may be associated with the stress whitening developed in this sample as a result of microvoid formation. The values obtained show reasonable agreement between the two methods.

For low draw ratio samples and also for a number of those annealed particularly from the second set of rods, the value of  $\alpha_{\parallel}$  is positive and is found to decrease in value as the temperature falls. In these cases it is necessary to re-examine the validity of equation (1). In the application to high draw ratio samples the value of  $\alpha_0$  is taken to be a constant, independent of temperature over the range of measurement involved. This is a reasonable assumption where the chain axis direction of the crystalline component provides the major proportion of the expansivity, since the crystal  $c$ -axis expansion coefficient is small and does not vary greatly with temperature. For example, the  $c$ -axis expansion coefficient derived from measurements by Davis, Eby and Colson<sup>6</sup> on

polyethylene samples does not change significantly in the temperature range considered. However, where there is a substantial contribution from the amorphous or transverse crystalline components, this assumption is no longer valid. Again taking polyethylene, the polyethylene  $a$ -axis expansion coefficient varies between  $221 \times 10^{-6} \text{ K}^{-1}$  at 10°C and  $160 \times 10^{-6} \text{ K}^{-1}$  at -50°C while the  $b$ -axis coefficient varies between  $54.3 \times 10^{-6} \text{ K}^{-1}$  at 10°C and  $62.5 \times 10^{-6} \text{ K}^{-1}$  at -50°C. Consequently whenever the  $c$ -axis (for polyethylene) is not predominantly aligned along the direction of draw or the crystalline content is insufficient for this to provide the major component in this direction then the corresponding intrinsic expansion coefficient  $\alpha_0$  will be temperature dependent. Account will then need to be taken of the relative contributions from the amorphous and crystalline regions. It is then necessary to put equation (1) in the form

$$\alpha_{\parallel} - (\alpha_{\parallel}^0) = \frac{B}{T} \left[ \frac{T}{E} \frac{dE}{dT} - 1 \right] \quad (2)$$

where  $(\alpha_{\parallel}^0)_{\parallel}$  is not independent of temperature.

In order to examine the validity of equation (2) it is necessary to establish the temperature dependence of  $(\alpha_{\parallel}^0)_{\parallel}$ .

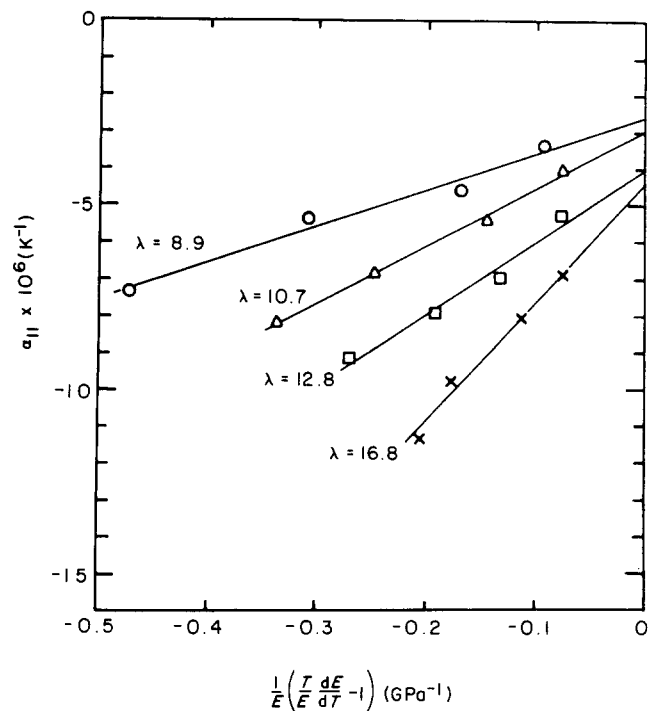


Figure 10 Variation of the expansion coefficient parallel to the draw direction with the modulus function (see text) for samples from set 1

Table 2 Comparison between direct shrinkage stress measurements and values derived from thermal expansion results for polypropylene die drawn rods

Draw ratio	$B$ (MPa/K)	$B \times T$ at 115°C (MPa)	Intercept $\alpha_0 \times 10^6$ ( $\text{K}^{-1}$ )	Shrinkage stress at 115°C (MPa)
8.9	0.010	3.9	-2.6	5.7
10.7	0.015	6.0	-3.0	6.0
12.7	0.019	7.6	-4.1	10.1
16.8	0.032	12.4	-4.5	7.4

We will propose that this can be obtained by measuring the temperature dependence of  $\alpha_{\perp}$ . The essence of our argument is that the temperature dependence of  $(\alpha_{T_1}^0)_{\parallel}$  can be related to the temperature dependence of  $\alpha_{\perp}$  by modelling the structure in the absence of a shrinkage force. This involves calculations similar to those proposed for the explanation of the *total* thermal expansion behaviour by Capiati and Porter<sup>7</sup>, and Choy and Chen and Ong<sup>4</sup>, but differing in detail in some respects by more explicit recognition of the difference in coupling in the parallel and perpendicular directions. A key experimental observation is that the temperature dependence of  $\alpha_{\perp}$  is to a good approximation identical in all samples, irrespective of draw ratio or annealing treatment. This result suggests that it will be reasonable to attempt to relate the temperature dependence of  $(\alpha_{T_1}^0)_{\parallel}$  to the temperature dependence of  $\alpha_{\perp}$ .

Although a final theoretical treatment should be based on a detailed structural model, we can proceed on the basis that the final values of the expansion coefficients of the structure parallel and perpendicular to the draw direction must be linear combinations of the parallel and perpendicular crystal components  $\alpha_{\parallel}^c$  and  $\alpha_{\perp}^c$  with further contributions from the amorphous regions,  $\alpha^a$ . For the present purposes the amorphous region is considered to be isotropic.

We then have

$$\alpha_{\parallel}^0 = a\alpha_{\parallel}^c + b\alpha_{\perp}^c + c\alpha^a \quad (3)$$

$$\alpha_{\perp} = d\alpha_{\parallel}^c + e\alpha_{\perp}^c + f\alpha^a \quad (4)$$

where  $a$ ,  $b$ ,  $c$ ,  $d$ ,  $e$  and  $f$  are weighting functions determined by various structural parameters involving the moduli and proportional parts of the various components.

To establish a simple relationship between the temperature dependences of  $\alpha_{\parallel}^0$  and  $\alpha_{\perp}$  we now make two further assumptions. First, we consider that the temperature dependence of  $\alpha_{\parallel}^c$  is very small so that

$$\frac{\partial \alpha_{\parallel}^0}{\partial T} = b \frac{\partial \alpha_{\perp}^c}{\partial T} + c \frac{\partial \alpha^a}{\partial T}$$

and

$$\frac{\partial \alpha_{\perp}}{\partial T} = e \frac{\partial \alpha_{\perp}^c}{\partial T} + f \frac{\partial \alpha^a}{\partial T}$$

Secondly, we note the experimental observation that  $\partial \alpha_{\perp} / \partial T$  is identical for all samples to a good approximation. This result implies that

$$\frac{\partial \alpha_{\perp}^c}{\partial T} \propto \frac{\partial \alpha^a}{\partial T}$$

to a similar approximation. Hence both the parallel and perpendicular expansivity variations are mainly determined by the perpendicular crystal variability term so that we may write

$$\frac{\partial \alpha_{\parallel}^0}{\partial T} = q \frac{\partial \alpha_{\perp}^c}{\partial T} = \frac{q}{s} \frac{\partial \alpha_{\perp}}{\partial T}$$

Hence

$$(\alpha_{T_2})_{\parallel} = (\alpha_{T_1})_{\parallel} + \frac{q}{s} \int_{T_1}^{T_2} \frac{\partial (\alpha_{T_1})_{\perp}}{\partial T} dT \quad (5)$$

where  $q$  and  $s$  are structural factors allowing for the combined effects of the crystalline and amorphous contributions in the respective directions. From the form of the equations  $q/s$  will be unity for isotropic material but will decrease as drawing proceeds. Where some amorphous orientation is involved it would be expected that an amorphous orientation factor would be involved in the  $\alpha^a$  contributions to  $q$  and  $s$ .

Equation (5) now predicts that the basic temperature variability of the parallel coefficient can be determined from the temperature variability in the perpendicular direction. The variation of the perpendicular component with temperature can be seen in *Figures 5, 6 and 7*. These indicate the large changes in level involved but, although there is some scatter, they show an essentially linear relationship with temperature which varies only slightly between draw ratios and is similar both before and after annealing. The integral in equation (5) can then be replaced by a constant value, which for these measurements is  $1.2 \times 10^{-6} \text{ K}^{-1}$  per degree so that equation (5) now becomes

$$(\alpha_{T_2})_{\parallel} = (\alpha_{T_1})_{\parallel} + q/s \times 1.2 \times 10^{-6} \times (T_2 - T_1) \quad (6)$$

In this paper we will consider two possible models for the structure, which follow closely our own previous research and that of other workers. For low draw ratios, the structure of the drawn polypropylene is close to a parallel lamellae texture of regularly spaced alternating blocks of crystalline and amorphous material. A calculation in the Appendix shows that for this structure

$$q/s = 2/3(1 - v)$$

where  $v$  is the crystalline volume fraction.

For high draw ratios, the modulus approaches an appreciable fraction of the crystal modulus. This result is similar to that for high modulus polyethylene, where the mechanical behaviour has been interpreted in terms of an intercrystalline bridge model, with crystal bridges linking adjacent crystalline blocks. In a simple mechanical model these bridges form a continuous crystalline phase in parallel with the alternating blocks of crystalline and amorphous material. Although there is no structural evidence for crystalline bridges in polypropylene we have adopted a similar model. This gives

$$\frac{q}{s} = \frac{2}{3}(1 - v_b) \frac{E_a}{E_{\parallel}^s}$$

where  $E_{\parallel}^s$  is the modulus of the model along the draw direction and  $v_b$  is the intercrystalline bridge volume fraction.

Assumptions introduced during the derivation will restrict the use of these values but they indicate declining values as crystallinity and modulus increase. Alternatively if it is assumed that the annealing process at the highest temperature (130°C) is sufficient to reduce the internal stresses to zero we can use equation (6) to derive a value

for  $q/s$  from a plot of  $\alpha_{\parallel}$  against temperature. This equation predicts a straight line of slope

$$(q/s)\partial\alpha_{\parallel}/\partial T$$

The results for the set 2 samples are plotted in *Figure 9*. Within the temperature range considered there is a reasonably linear relationship although at the lowest temperature the lower draw ratios show a reduced rate of fall as might be expected from the increasing rigidity in the amorphous regions. The corresponding values for  $q/s$  are shown in *Table 3*.

These values show, as expected, that the temperature contribution to  $\alpha_0$  is very large at the lower draw ratios. Ideally the same value of  $q/s$  for a particular draw ratio could be applied to obtain a correction factor for the measurements taken before annealing but unfortunately, evidence from other sources indicates that the structure is modified by annealing and hence we must assume changes in  $q/s$ . Studies by Clements *et al.*<sup>8</sup> on polyethylene have shown that one effect of annealing is to reduce the longitudinal crystal thickness with a corresponding decrease in modulus. Small-angle X-ray examination of the present samples has shown more prominent arc formation after annealing at 130°C thus confirming structural changes. However, since the annealing process will tend to reduce the degree of order, the  $q/s$  values can still be used to provide a temperature correction factor but the subsequent derived values from the slopes will then only indicate an upper limit for the shrinkage stress and these values are shown in *Table 4*.

The annealing process for the samples considered previously was carried out with the rods free to shrink and hence with any stresses present able to deform the structure. Brief measurements were made with two samples from set 1 where the rods were held at constant length during annealing at 130°C. The results are shown in *Table 5*.

These measurements indicate that under restraint the stresses are not relieved completely (or are partially re-established on cooling) and that, for the higher draw ratio, the crystalline component provides the important part of the structure in the draw direction.

## CONCLUSIONS

Measurements of the thermal expansion coefficients of die drawn polypropylene copolymer rods over a temperature

**Table 3** Variation of the structural factor ratio  $q/s$  (see text) with draw ratio as determined from the variation of  $\alpha_{\parallel}$  with temperature

Draw ratio	2.4	6.2	9.6	12.6
$q/s$	0.82	0.78	0.37	0.082

**Table 4** Maximum values of  $B$  derived from a temperature correction based on zero stress after annealing at 130°C

Draw ratio	$B_{\max}$ (MPa/K)	$B_{\max} \times T$ at 115°C (MPa)
6.2	0.038	14.8
9.6	0.038	14.8
12.6	0.022	8.5

**Table 5** Effect of the annealing conditions on the axial thermal expansion coefficient

Mean temperature (°C)	Draw ratio	Initial value	Axial thermal expansion coefficient $\times 10^6$	
			Value after free annealing at 130°C	Value after restrained annealing at 130°C
2.4	6.4	-1.2	14.1	10.4
-13.4	6.4	-0.8	11.6	8.7
-29.9	6.4	-0.6	10.1	7.6
-47.2	6.4	0.0	9.1	7.2
2.4	8.9	-7.4	0.2	-3.5
-13.4	8.9	-5.4	1.7	-2.6
-29.9	8.9	-4.6	1.6	-1.4
-47.2	8.9	-3.4	1.6	-0.6

range from -50°C to +10°C have shown mainly low negative values along the draw direction with high positive radial values. The axial values decrease with increasing draw ratio but the absolute magnitudes, both positive and negative, increase with temperature.

After annealing, these axial values become predominantly positive. Interpretation based on the relationship between radial and axial temperature effects is shown to explain the results on the basis of the presence of reasonable internal stresses introduced at drawing as proposed in an earlier paper by Orchard, Davies and Ward<sup>2</sup>.

## REFERENCES

- Choy, C. L., Chen, F. C. and Young, K. J. *Polym. Sci., Polym. Phys. Edn.* 1981, **19**, 335
- Orchard, G. A. J., Davies, G. R. and Ward, I. M. *Polymer* 1984, **25**, 1203
- Coates, P. D. and Ward, I. M. *Polymer* 1979, **20**, 1553
- Choy, C. L., Chen, F. C. and Ong, E. L. *Polymer* 1979, **20**, 1191
- Struick, L. C. E. *Polym. Eng. Sci.* 1978, **18**, 798
- Davis, G. T., Eby, R. K. and Colson, J. P. *J. Appl. Phys.* 1970, **41**, 4316
- Capiati, N. J. and Porter, R. S. *J. Polym. Sci., Polym. Phys. Edn.* 1977, **15**, 1427
- Clements, J., Jakeways, R., Longman, G. W. and Ward, I. M. *Polymer* 1979, **20**, 295
- Williams, T. J. *Mater. Sci.* 1973, **8**, 59

## APPENDIX

To obtain a theoretical value for the  $q/s$  term in equation (5) it is necessary to adopt a structural model for the polymer and to make certain assumptions about the relationship between the temperature coefficients of the amorphous and crystalline expansivities. For the isotropic material  $q/s$  must be unity and during the early stages where crystallite orientation is incomplete and is blocks are progressively pulled out of the structure and aligned along the draw direction involves intermediate stages where crystallite orientation is incomplete and is expressed in terms of an orientation factor  $\langle P_2(\cos \theta) \rangle = \frac{1}{2}(3\langle \cos^2 \theta \rangle - 1)$  where  $\theta$  is the angle between the major axis of the structural unit and the draw direction. Expressions for the parallel and perpendicular expansion coefficients have been given by Choy, Chen and Ong<sup>4</sup> based on a composite of an aggregate crystalline form combined with an isotropic amorphous phase. The

resulting equations are

$$\alpha_{\parallel} = \frac{v}{3}(1 + 2P_2)\alpha_{\parallel}^c + \frac{2v}{3}(1 - P_2)\alpha_{\perp}^c + (1 - v)\alpha^a \quad (A1)$$

$$\alpha_{\perp} = \frac{v}{3}(1 - P_2)\alpha_{\parallel}^c + \frac{v}{3}(2 + P_2)\alpha_{\perp}^c + (1 - v)\alpha^a \quad (A2)$$

If we now assume that to a good approximation the temperature coefficients of the amorphous and the perpendicular crystallite component are proportional, i.e.

$$\frac{\partial \alpha^a}{\partial T} = k \frac{\partial \alpha_{\perp}^c}{\partial T} \quad (A3)$$

where  $k$  is constant, we obtain

$$q/s = \left[ \frac{2v}{3}(1 - P_2) + k(1 - v) \right] / \left[ \frac{v}{3}(2 + P_2) + k(1 - v) \right] \quad (A4)$$

If we further assume  $\alpha^a$  to be equal to the mean crystal value then

$$\alpha^a = (2\alpha_{\perp}^c + \alpha_{\parallel}^c)/3 \quad (A5)$$

and  $k = 2/3$

to give

$$q/s = \frac{2(1 - vP_2)}{2 + vP_2} \quad (A6)$$

For many polymers the orientation is effectively complete and hence  $P_2 = 1$  at fairly low draw ratios. Williams<sup>9</sup> found this to occur for extruded polypropylene by draw ratio 5 and hence we need to adopt a different model above this level.

We will consider the model to consist of a fully aligned crystalline component in series with an isotropic amorphous component along the draw direction with both components sheathed by a third component in parallel. The third component may be either amorphous, giving effectively oriented crystalline units embedded in an amorphous matrix, or crystalline, resulting in an intercrystalline bridge configuration. For simplicity to maintain symmetry in the perpendicular directions the model is taken to have a square cross section as shown in Figure 11. Mathematically the structure will be treated as a parallel-series model in the draw direction and a series-parallel model in the perpendicular direction. Subscripts T, a, c and s will be used for the various parameters of the entire structure, the amorphous, the crystalline and the sheath components respectively.

If we now consider the balance of forces resulting from a small temperature change we can relate the modulus  $E$  to the thermal expansion coefficient. The force  $F$  between the top and bottom faces along the draw direction is given by

$$F = \frac{E_T A_T \Delta L_T}{L_T} = \frac{E_s (A_T - A_c) \Delta L_s}{L_s} + \frac{A_c (\Delta L_a + \Delta L_c)}{L_a/E_a + L_c/E_c}$$

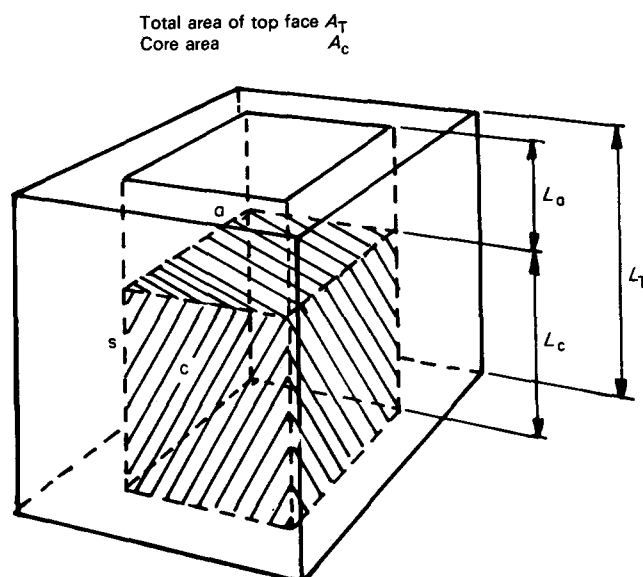


Figure 11 Core/sheath model element used in the calculations

where

$$E_T = \frac{(A_T - A_c) E_s}{A_T} + \frac{A_c L_T}{A_T L_a/E_a + L_c/E_c}$$

Since

$$\alpha = \frac{1}{L} \frac{dL}{dT}$$

the  $\Delta L$  terms can be replaced by  $\alpha \Delta T$  to give

$$\alpha_T = \alpha_s + A_c (L_a \alpha_a - L_c \alpha_c - L_T \alpha_s)$$

$$\times \left[ \left( \frac{L_a}{E_a} + \frac{L_c}{E_c} \right) (A_T - A_c) E_s + A_c L_T \right]^{-1}$$

If the sheath is amorphous we have  $E_a = E_s$  with the crystalline volume fraction  $v$  given by

$$v = \frac{A_c L_c}{A_T L_T} = \frac{A_c (L_T - L_a)}{A_T L_T}$$

and  $\alpha_s = \alpha_a$  to give

$$\alpha_{\parallel} = \alpha_a + \frac{v(1 - v_a)}{(1 - v_a) + v v_a (E_a/E_c - 1)} (\alpha_{\parallel}^c - \alpha_a) \quad (A7)$$

here  $v_a$  is the amorphous sheath volume fraction.

If the sheath is crystalline we have  $E_c = E_s$  with the crystalline volume fraction  $v$  given by

$$v = \frac{A_T L_T - A_c L_a}{A_T L_T}$$

and the intercrystalline bridge volume fraction

$$v_b = \frac{A_T - A_c}{A_T}$$



with  $\alpha_s = \alpha_c (= \alpha_{\parallel}^c)$  to give

$$\alpha_{\parallel} = \alpha_{\parallel}^c + \frac{(1-v)(1-v_b)}{(1-v_b) + (1-v)v_b \left[ \frac{E_c}{E_a} - 1 \right]} (\alpha_a - \alpha_{\parallel}^c) \quad (\text{A8})$$

In the absence of a sheath, i.e. for  $v_a = 0 = v_b$  these both reduce to

$$\alpha_{\parallel} = v\alpha_{\parallel}^c + (1-v)\alpha_a \quad (\text{A9})$$

Similarly if we consider the perpendicular direction in a similar manner with the central slice of thickness  $A_c^{1/2}$  containing the parallel components in the series-parallel configuration we have for this slice

$$F = E_B A_T^{1/2} L_T \Delta(A_c^{1/2}) / A_c^{1/2} \\ = \frac{E_s (A_T^{1/2} - A_c^{1/2}) L_s \Delta(A_c)^{1/2}}{A_c^{1/2}} + \frac{E_a A_c^{1/2} L_a \Delta(A_c)^{1/2}}{A_c^{1/2}} \\ + \frac{E_c A_c^{1/2} L_c \Delta(A_c)^{1/2}}{A_c^{1/2}}$$

where

$$E_B = \frac{(A_T^{1/2} - A_c^{1/2}) L_s}{A_T^{1/2} L_T} E_s + \frac{A_c^{1/2} L_a}{A_T^{1/2} L_T} E_a + \frac{A_c^{1/2} L_c}{A_T^{1/2} L_T} E_c$$

the modulus of the composite slice. Hence

$$\alpha_B = \alpha_s + [E_a A_c^{1/2} L_a (\alpha_a - \alpha_s) + E_c A_c^{1/2} L_c (\alpha_c - \alpha_s)] \\ \times [(A_T^{1/2} - A_c^{1/2}) L_s E_s + A_c^{1/2} L_a E_a + A_c^{1/2} L_c E_c]^{-1}$$

Again for the amorphous sheath this gives for the slice with  $\alpha_s = \alpha_a$

$$\alpha_B = \alpha_a + \frac{v(1-v_a)^{1/2}}{[(1-v_a) - v(1-v_a)^{1/2}] \frac{E_a}{E_c} + v(1-v_a)^{1/2}} (\alpha_{\perp}^c - \alpha_a)$$

Combining this with the remaining sheath components in series then gives

$$\alpha_{\perp} = \alpha_a + \frac{v(1-v_a)}{[(1-v_a) - v(1-v_a)^{1/2}] \frac{E_a}{E_c} + v(1-v_a)^{1/2}} (\alpha_{\perp}^c - \alpha_a) \quad (\text{A10})$$

Similarly for the crystalline sheath the value for the slice with  $\alpha_s = \alpha_c$

$$\alpha_B = \alpha_{\perp}^c + \frac{(1-v)}{[(1-v_b)^{1/2} - (1-v)] \frac{E_c}{E_a} + (1-v)} (\alpha_a - \alpha_{\perp}^c)$$

and combining this with the remaining sheath components in series then gives

$$\alpha_{\perp} = \alpha_{\perp}^c + \frac{(1-v)(1-v_b)^{1/2}}{[(1-v_b)^{1/2} - (1-v)] \frac{E_c}{E_a} + (1-v)} (\alpha_a - \alpha_{\perp}^c) \quad (\text{A11})$$

Again in the absence of a sheath, i.e. for  $v_a = 0 = v_b$  these both reduce to

$$\alpha_{\perp} = \left[ 1 - \frac{(1-v)}{v \frac{E_{\perp}^c}{E_a} + (1-v)} \right] \alpha_{\perp}^c + \frac{(1-v)}{v \frac{E_{\perp}^c}{E_a} + (1-v)} \alpha_a \quad (\text{A12})$$

where  $E_{\perp}^c$  is the transverse modulus of the crystalline component.

To obtain a value for  $q/s$  it is now necessary to combine equations (A7) and (A10) for the amorphous sheath, equations (A8) and (A11) for intercrystalline bridges or equations (A9) and (A12) for the simple structure with alternate crystalline and amorphous regions in series. In each case the temperature coefficients of the amorphous and the perpendicular crystalline regions must be assumed to be related as in equations (A3) or (A5).

Since the crystalline modulus values are much greater than those obtained for the amorphous regions the final  $q$  and  $s$  values can be simplified to give the following expressions based on the substitution from equation (A3):

From equation (A7)

$$q = k \left[ 1 - \frac{v(1-v_a)}{(1-v_a) + v v_a \left[ \frac{E_a}{E_{\parallel}^c} - 1 \right]} \right] \rightarrow k \left[ 1 - \frac{v}{1 - \frac{v v_a}{1-v_a}} \right]$$

From equation (A10)

$$s = k + (1-k) \frac{v(1-v_a)^{1/2}}{[(1-v_a) - v(1-v_a)^{1/2}] \frac{E_a}{E_{\perp}^c} + v(1-v_a)^{1/2}} \\ \rightarrow k + (1-k) = 1$$

From equation (A8)

$$q = \frac{k(1-v)(1-v_b)}{(1-v_b) + (1-v)v_b \left[ \frac{E_{\parallel}^c}{E_a} - 1 \right]} \rightarrow \frac{k(1-v_b) \frac{E_a}{E_{\parallel}^c}}{v_b \frac{E_{\parallel}^c}{E_a}} \rightarrow k(1-v_b) \frac{E_a}{E_{\parallel}^s}$$

where  $E_{\parallel}^s$  is the sample modulus in the draw direction.

From equation (A11)

$$s = 1 + (k-1) \frac{(1-v)(1-v_b)^{1/2}}{[(1-v_b)^{1/2} - (1-v)] \frac{E_{\perp}^c}{E_a} + (1-v)} \\ \rightarrow 1 + (k-1) \frac{(1-v)(1-v_b)^{1/2} \frac{E_a}{E_{\perp}^c}}{(1-v_b)^{1/2} - (1-v)}$$

From equation (A9)  $q = k(1-v)$

From equation (A12)

$$s = 1 + (k-1) \frac{1-v}{v \frac{E_{\perp}^c}{E_a} + (1-v)} \rightarrow 1 + (k-1) \frac{1-v}{v} \frac{E_a}{E_{\perp}^c}$$

Hence for the fully oriented samples in which we have  $1 > 1 - v_a > v > v_b$  with  $v \geq 0.5$ , the value of the  $s$  factor is

close to unity and the  $q/s$  ratios will approximate to the following values for  $k=2/3$  (equation (A5))

$$q/s = \frac{2}{3} \left[ 1 - \frac{v}{1 - \frac{vv_a}{1 - v_a}} \right] \quad (\text{amorphous sheath})$$

$$q/s = \frac{2}{3} (1 - v_b) \frac{E_a}{E_s} \quad (\text{intercrystalline bridges})$$

$$q/s = \frac{2}{3} (1 - v) \quad (\text{alternating crystalline and amorphous regions})$$

Work by Choy *et al.*<sup>4</sup> indicates that the loose structure in the amorphous regions allows greater thermal movement so that  $k$  exceeds the value of  $2/3$  and may be greater than unity.